Assessment offlutter speed onthe long span bridges

M. Papinutti[1], J. Kramer Stajnko[1], R. Jecl[1], A. Štrukelj[1], M. Zadravec[2], J.A. Jurado[3]
[1]*Faculty of Civil Engineering, University of Maribor, Slovenia.*
[2]*Faculty of Mechanical Engineering, University of Maribor, Slovenia.*
[3]*School of Civil Engineering, University of Coruña, Campus de Elviña, Spain.*

Abstract

In the present paper is shown how to calculate flutter speed on example of Great Belt East Bridge. Two numerical approaches are shown for prediction of the aeroelastic phenomena on bridges. In CFD simulation turbulence model based on Reynolds Average Navies Stokes (RANS) approach, two-equation SST turbulent model was chosen. Although SST turbulent model need more computer resources compared to k-ω and k-ε models, it is still affordable with multi-processing personal computers. In this paper extracted flutter derivatives in force vibration procedure is shown. Flutter derivatives are later used in hybrid method of flutter. Final flutter speed was calculated basison flutter derivatives from Fluid Structure Interaction extraction and experimental extraction. Flutter velocity was also determined with free vibration of deck at the middle of the bridge. Deck section of unit length was clamped in to springs and dampers. Flutter speed was reached with time increasing of wind speed until large oscillations occurred. In paper is shown general procedure how to formulate fluid structure interaction and necessary stapes for flutter analysis of bridge. Numerically extracted flutter derivatives are compared basis of final flutter speed to experimental measurements of deck section.

Keywords: bridge aeroelasticy, long span bridge, flutter derivatives, numerical simulation, fluid structure interaction, computational fluid dynamics.

1 Bridge aeroelasticy

The aeroelastic stability of line-like slender structures, like suspension and cable-stay bridges is verified by calculatingof a critical wind speed. Light structures are sensitive to aeroelastic phenomena like galloping, divergence and flutter. Therefore the aeroelastic properties of the bridge deck section are needed and are commonly determined in wind tunnel tests. For bridge structural parameters have to be calculated andfurthermore moreaeroelastic parameters must be measured. In phase of projecting flutter speed can be estimated fully with computationa approach. In general,aeroelastic studies are time consuming and quicker calculations could be done with Fluid Structure Interaction (FSI)analysis. For aeroelasticresponse in hybrid method we need linearized flutter derivatives to close dynamic equations and dynamic response of structure. Hybrid method is very useful tool for optimization, sensitivity analysis and flutter speed calculations. Multimodal response could be captured, but in our example we captured only vertical and torsional degree of freedom. Two different methods exist forextraction of flutter derivatives, free and forced vibration testing. For our investigation force vibration test were simulated with commercial software Ansys 14 for Computational Fluid Dynamics or CFD. A presentation of extraction of flutter derivatives, will be presented by FSI simulation with force vibration test. Results of flutter derivatives will be imported in hybrid method for calculating of flutter speed. Second numerical possibility is to cut unit length of bridge deck segment at one fourth or one half of the bridge and investigate aeroelastic response.Segment we clamp in springs, dampers and assign proper modal mass for chosen frequencies. Under different wind velocities we observe oscillations of the deck. Independent from hybrid results in frequency domain, a time domain FSI is calculated for clamped deck section.

2 Flutter

It is shown that the fundamental torsional vibration mode dominantly involves to the flutter instability for bluff cross sections like low slenderness ratio (B/D) rectangular sections or H-shape sections or stiffened truss sections. The flutter instability [1] is known as the torsional flutter, as the case of Tacoma Narrow failure. Whereas the fundamental torsional mode and any first symmetric or asymmetric heaving mode usually couple mechanically at single frequency with the streamlined cross sections as known as the coupled flutter or the classical flutter. Coupled flutter was studied previously on aerodynamics of airplane's airfoil wings and later developed for bridge line-like structures. It is interesting that coupled flutter has occurred in case of the Great Belt East Bridge with streamlined deck section. Following chapter will describe basic equations of flutter, based on which later flutter speed is calculated.

2.1 Equations of flutter

Aeroelastic forces are linearized as a function of the movements and speeds of the board, analogously to the forces occurring in the Theodorsen theory,[2]. The expressions for lift F_z and the moment F_θ forces are:

$$F_z = \frac{1}{2}\rho V^2 B \left[K H_1^* \left(\frac{\dot{z}}{V}\right) + K H_2^* B \left(\frac{\dot{\theta}}{V}\right) + K^2 H_3^*(\theta) + K^2 H_4^* \left(\frac{z}{B}\right) \right] \quad (1)$$

$$F_\theta = \frac{1}{2}\rho V^2 B^2 \left[K A_1^* \left(\frac{\dot{z}}{V}\right) + K A_2^* B \left(\frac{\dot{\theta}}{V}\right) + K^2 A_3^*(\theta) + K^2 A_4^* \left(\frac{z}{B}\right) \right] \quad (2)$$

where$V$ is the average wind speed, B the width of the section, ρ is the density of air and $K = \omega B/V$ is the reduced frequency. Circular frequency is $\omega = 2\pi f$ in units $[rad/s]$ and the frequency f units are in $[1/s]$. So called *flutter derivatives*H_i^*, $A_i^*$with $i = 1 \ldots 4$ are functions ofreduced frequency K. Moment force M_θ, along X-axis that produces torsional rotation along the deck. Lift force F_z causes lift of the deck and is important for flutter coupling between rotational and vertical movement. Drag forces $F_y$is neglected for simplification and small participation factors to flutter speed, but can be important for long suspension, [3].

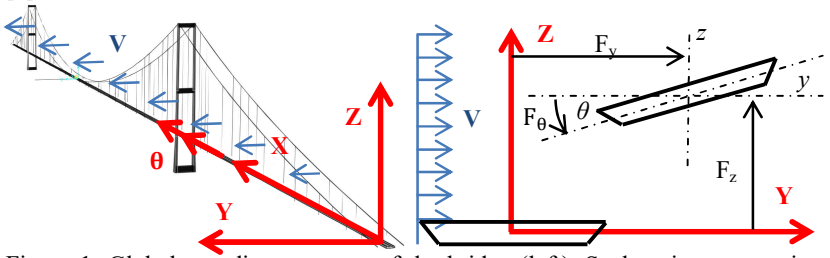

Figure 1: Global coordinate system of the bridge (left), Scalan sign convention used in the analysis of the flutter instability (right).

Classical flutter occurs when vertical and torsional vibrations have natural frequencies close together and larger mass is activated in each mode shape.Heaving and torsional motion equations of the flutter, where z is vertical motion and θ torsional motion can be expressed with following expressions:

$$M_z \cdot \ddot{z}(t) + C_z \cdot \dot{z}(t) + K_z \cdot z(t) = \frac{1}{2}\rho V^2 B L \left[K H_1^* \frac{\dot{z}}{V} + K H_2^* \frac{B\dot{\theta}}{V} + K^2 H_3^* \theta + K^2 H_4^* \frac{z}{B} \right] \quad (3)$$

$$M_\theta \cdot \ddot{\theta}(t) + C_\theta \cdot \dot{\theta}(t) + K_\theta \cdot \theta(t) = \frac{1}{2}\rho V^2 B^2 L \left[K A_1^* \frac{\dot{z}}{V} + K A_2^* \frac{B\dot{\theta}}{V} + K^2 A_3^* \theta + K^2 A_4^* \frac{z}{B} \right] \quad (4)$$

whereM_{i} is mass, C_{i} is structural damping and K_{i} is stiffness of mode i.Introducing$\overline{K_i} = B\omega_{\mathrm{i}}/V$, non-dimensional time variable $s = \frac{Vt}{B}$, first order$\dot{s}$ and second-order $\ddot{s}$ differentials of time we get equationsof flutter:

$$\left[-K^2 + 2i\overline{K}_z\xi_{\mathrm{z}}K + \overline{K}_z^2 - \frac{i\rho B^2K^2}{2M_{\mathrm{z}}}H_1^* - \frac{\rho B^2K^2}{2M_{\mathrm{z}}}H_4^*\right]\frac{1}{B}\mathrm{z}_0 - \left[+\frac{\rho B^2iK^2}{2M_{\mathrm{z}}}H_2^* + \frac{\rho B^2K^2}{2M_{\mathrm{z}}}H_3^*\right]\theta_0 = 0 \tag{5}$$

$$\left[-\frac{i\rho B^4K^2}{2M_\theta}A_1^* - \frac{\rho B^2K^2}{2M_{\mathrm{z}}}A_4^*\right]\frac{1}{B}\mathrm{z}_0 + \left[-K^2 + 2i\xi_\theta\overline{K}_\theta\mathrm{K} + \overline{K}_\theta^2 - \frac{\rho B^4iK^2}{2M_\theta}A_2^* - \frac{\rho B^2K^2}{2M_\theta}A_3^*\right]\theta_0 = 0 \tag{6}$$

Solution of system is in determinant which must be zero.The determinant of, eqn. (5,6) can be expandedand groupedby real and imaginary part as follow:

$$\mathrm{Det}[H] = \Delta_1 + \Delta_2 i = 0 \tag{7}$$

As a result, the flutter motion differential equations of heaving-torsional system have been transformed to two polynomial equations with ω-variable. Critical state of circular frequency or flutter frequency is when sum of real and imaginary part are zero,[4].

2.2 Extraction of flutter derivatives by force vibration procedure

Considering flutter as anaeroelastic stability problem, the motion of the bridge deck at the stability border is assumed to be a sinusoidal motion with constant amplitude. For forced vibration tests of the unit length deck insmaller scale is used. Pure sinusoidal oscillation according to the mathematical assumption can be realized. The bridge deck involves two types of deformation: bending and twist. Based on the analytical theory of Theodorsen,a modified theory is introduced by Starossek [5], [6].

Mathematical expressionsare used for determination ofmodal parameters [7]. The harmonic behaviour of the system is introduced, by the use of expression for sinusoidal motion and exponential damping in eqn. (8):

$$\begin{Bmatrix}\mathrm{y}(t)\\ \mathrm{z}(t)\\ \theta(t)\end{Bmatrix} = \begin{Bmatrix}\tilde{\mathrm{y}}\\ \tilde{\mathrm{z}}\\ \tilde{\theta}\end{Bmatrix} e^{i\omega t} \tag{8}$$

where$y(t)$ is sinusoidal lateral motion $[m]$, $z(t)$ vertical sinusoidal motion $[m]$ and $\theta(t)$ is rotation $[m]$, ω is the frequency $[rad]$, t is time variable $[s]$ and $\tilde{\mathrm{y}}$, $\tilde{\mathrm{z}}$ and $\tilde{\theta}$are amplitudes of lateral, vertical and rotational movement. The forces described by the lift and moment coefficients are expected to vary in a similar

way. A phase difference, between the motion and the load ψ is described by phase angle[*rad*]in eqn. (9(10).

$$C_L e^{i(\omega t-\psi_L)} = \left[KH_1^*\left(\frac{\dot{z}}{V}\right) + KH_2^* B\left(\frac{\dot{\theta}}{V}\right) + K^2 H_3^*(\theta) + K^2 H_4^*\left(\frac{z}{B}\right)\right] e^{i\omega t} \quad (9)$$

$$C_M e^{i(\omega t-\psi_M)} = \left[KA_1^*\left(\frac{\dot{z}}{V}\right) + KA_2^* B\left(\frac{\dot{\theta}}{V}\right) + K^2 A_3^*(\theta) + K^2 A_4^*\left(\frac{z}{B}\right)\right] e^{i\omega t} \quad (10)$$

Phase angles are between $0 < \psi < \pi/2$ and is calculated based on fitted sinusoidal curve to each of deck force and later phase difference between sinusoidal motion and movement is calculated in eqn. (11).

$$A_1^* = \mathrm{Im}\left(\frac{C_M B e^{-i\psi_M}}{K^2 \tilde{z}}\right) \quad A_2^* = \mathrm{Im}\left(\frac{C_M e^{-i\psi_M}}{K^2 \tilde{\theta}}\right) \quad A_3^* = \mathrm{Re}\left(\frac{C_M e^{-i\psi_M}}{K^2 \tilde{\theta}}\right)$$
$$A_4^* = \mathrm{Re}\left(\frac{C_M B e^{-i\psi_M}}{K^2 \tilde{z}}\right) \quad H_1^* = \mathrm{Im}\left(\frac{C_L B e^{-i\psi_L}}{K^2 \tilde{z}}\right) \quad H_2^* = \mathrm{Im}\left(\frac{C_L e^{-i\psi_L}}{K^2 \tilde{\theta}}\right) \quad (11)$$
$$H_3^* = \mathrm{Re}\left(\frac{C_L e^{-i\psi_L}}{K^2 \tilde{\theta}}\right) \quad H_4^* = \mathrm{Re}\left(\frac{C_L B e^{-i\psi_L}}{K^2 \tilde{z}}\right)$$

3.1.1 Phase angle

Phase angle is delay ofthe load from motion. Load and motion are correlated as expected, as a positive clock wise rotation results in a positive moment and an upward liftFigure 1. The time interval found in this particular case in Figure 2 is approximately 0.35*rad* for the lift and 0.12*rad* for moment. The phase difference is converted from time interval to radians as [8], eqn. (12):

$$\psi = \frac{2\pi \Delta t}{T} \quad (12)$$

Where Δt is the time interval of the phase shift.Considering equation (11), the unknown is the phase shift ψ, which can be found with the time interval between the motion and the load as shown in Figure 2.

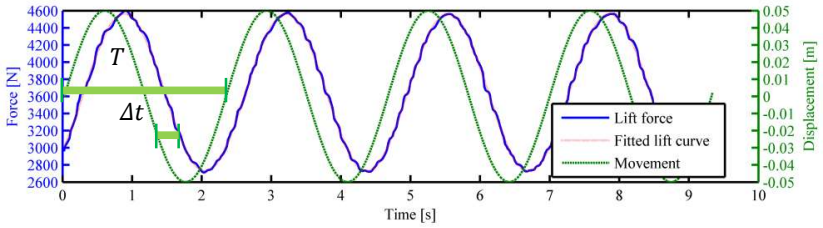

Figure 2:Lift force F_z and vertical oscillation z for illustration of the phase shift for the case with a reduced velocity $K = 10$ for force oscillation of frequency $\omega = 0.129\ 1/s$ and wind speed$V = 80\ ms^{-1}$.

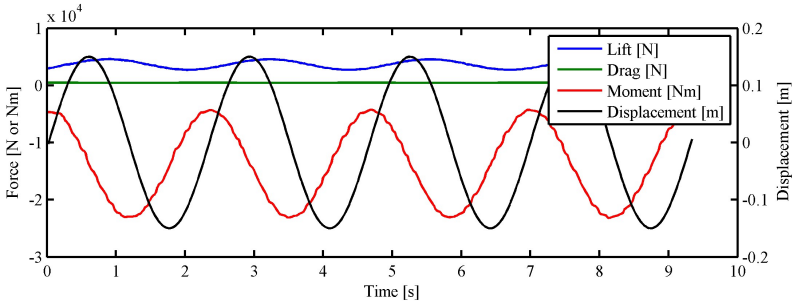

Figure 3: Aerodynamic forces for vertical oscillation$z_2 = 15m$,$K = 10$,$\omega = 0.129 l/s$,$V = 80 m/s$.

In example flutter derivatives for vertical motion $H_1^*, H_2^*, H_3^*, H_4^*$ and for rotational motion $A_1^*, A_2^*, A_3^*, H_4^*$ as a function of reduce frequencies K are calculated. Two different amplitudes were used for vertical force motion $z_1 = 0.05m$and $z_2 = 0.15m$. For rotation $\theta_1 = 5°$ and $\theta_2 = 15°$are used and compare with different phase angles. It is of the main importance to calculate phase angels and derivatives.Results forfour most important flutter derivatives are shown in Figure 1furthermore, phase angles and are listed in Table 1 and the differencesbetween amplitudes inTable 2.

Table 1: Phase shifts ψ for rotational oscillation $\theta_1 = 5°$ and vertical oscillation$z_1 = 5$ cm

Reduce frequency K		*1*	*3*	*6*	*10*	*15*
Frequency of oscillation		*1,290*	*0,430*	*0,215*	*0,129*	*0,086*
Lift	Rotational oscillation $\theta_1 = 5°$	1,03	0,95	0,65	0,35	0,19
Drag		-0,51	-0,26	0,05	0,16	0,19
Moment		0,39	0,17	0,16	0,12	0,09
Lift	Vertical oscillation $z_1 = 5$ cm	0,27	0,76	1,35	1,46	1,43
Drag		-1,44	-1,58	-1,38	-1,37	-1,39
Moment		-1,54	-1,54	-1,45	-1,44	-1,46

Table 2: Difference for different amplitudes of rotational θ_2/θ_1 and vertical z_2/z_1oscillation in [%]

Reduce frequency K		*1*	*3*	*6*	*10*	*15*
Lift	Rotation	-8,79%	0,15%	-0,21%	-0,67%	-1,39%
Drag		12,29%	-2,44%	4,99%	-2,74%	-2,17%
Moment		28,77%	0,77%	-0,19%	-0,13%	-0,01%
Lift	Vertical	-40,65%	0,88%	0,05%	0,04%	7,08%
Drag		1,25%	0,14%	0,34%	-0,02%	-8,70%
Moment		0,00%	0,00%	0,00%	0,00%	0,00%

3.1.2 Aerodynamic coefficients

Aerodynamic coefficients are calculated in first stage of CFD simulations. Aerodynamic coefficients for stationary and non-stationary simulations are very similar but not the same. Usually stationary solution underestimates forces on deck. Aerodynamic non-stationary coefficients are result of average force in time. For our investigation aerodynamic forces on deck are calculated from stationary simulation. Drag aerodynamic coefficient$C_D = 0.044$, lift aerodynamic coefficient$C_L = 0.197$ and moment aerodynamic coefficient$C_M = 0.050$ are calculated from forces on deck section at wind speed $V = 80\ m/s$.

2.3 Flutter derivatives

The results are validated by comparison with wind tunnel tests, from ref.[9],focusing on the two-dimensional case.It is evident that amplitude does not significantly influencesthe results,it influences the most the drag force. Instabilities of extraction were noticed also at higher amplitudes of rotations, where vortex from leading traveling along the deck influenced the results. Flutter derivatives are compared to experimental data and itis possible to observe good agreement.The results are shown in Figure 4.

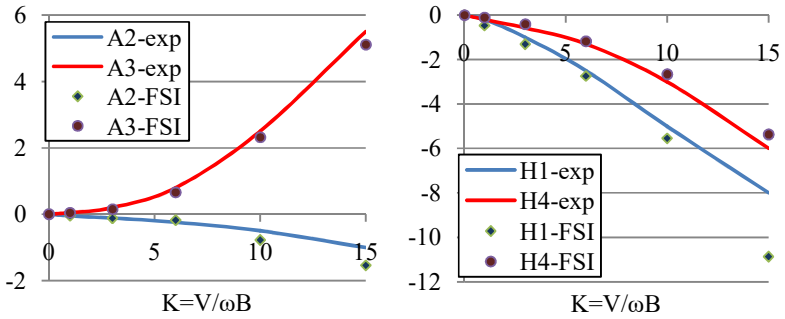

Figure 4:Extracted flutter derivatives from experiments and FSI calculated by force vibration test.

Beteragreement can be reached with 3D mesh, denser mesh and other, more accurate turbulence model.

3 Direct simulation of fluid structure interaction of flutter

Different possibilities of moving meshes are possible to define rigid body motion. Two examples of mathematical model are shown inFigure 5.

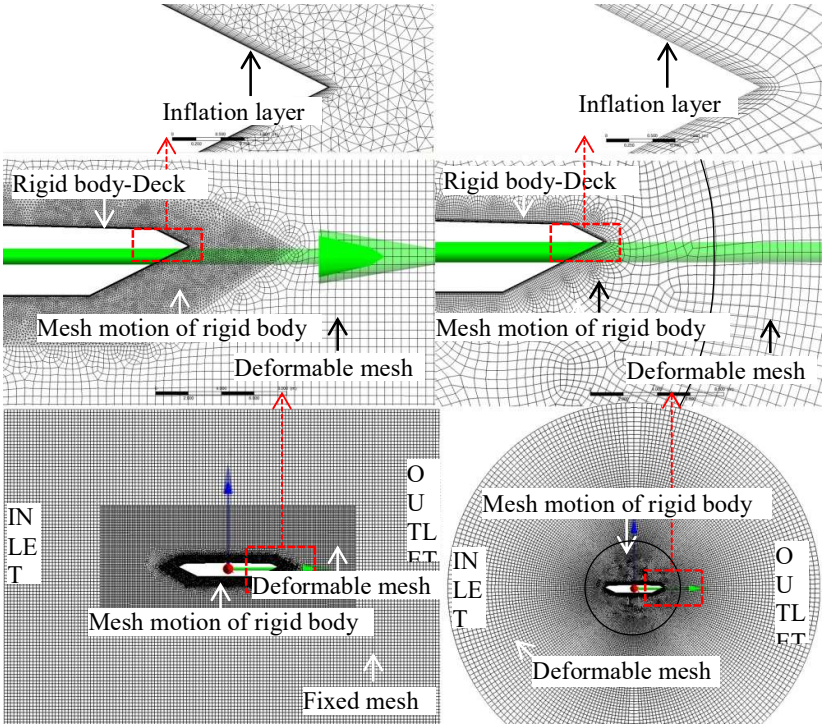

Figure 5:Different models for FSI analysis. Model for flutter derivatives extraction (left), direct FSI simulation of flutter (right).

3.1 Turbulence model

In RANS equations instantaneous fluctuations are modelled by closure model. Most popular are one and two equation models that are computationally cheap. The most economic approach is RANS flow modelling for computing complex turbulent industrial flows. RANS models are suitable for many engineering applications and typically provide the level of accuracy required. Since none of the models is universal, the most suitable turbulent model is important decision for in a given applications. It influences aerodynamic force which strongly influences mechanism of energy transfer in to motion, while dynamic turbulence force from vortex shedding does not have big influence on flutter.

More complex RANS is Shear Stress Turbulence model. The transition SST model is based on the coupling of the SST transport equations with two other transport equations, one for the intermittency and one for the transition onset criteria, in terms of momentum-thickness Reynolds number. An ANSYS empirical correlation covers standard bypass transition as well as flows in low free-stream turbulence environments. In addition, a very powerful option is

included to allow to enter own user-defined empirical correlation.It was used to control the transition onset momentum thickness Reynolds number equation, which was used to match results of flutter derivatives.Mesh of our investigation is three-dimensional, while boundary conditions are set in a way that symmetry condition defines equations to solve two-dimensionswhich is computationally cheaper[10]. Computation time is cheaper for 2D mesh and does not have a big influence for line-like structure computed in RANS models.

3.2 Mathematical model of FSI

For complete FSI structure interaction it is necessary to simulate all dynamical properties of the bridge at the observation point and all of the fluid motion around it. For extermination of the dynamical properties Finite Element Model FEM for calculation of frequencies and modal participations masses are needed. Fluid properties are calculated in stationary CFD analysis. Non-stationary simulation is important for determination of maximal and averaged Courant number, which is important for numerical stable solution. Finally FSI model is created from CFD file. In FSI simulation theareas of mesh deformation and boundary conditions of mesh deformations are determined. In Figure6 necessary steps for modelling of FSI of aeroelastic phenomena are described.

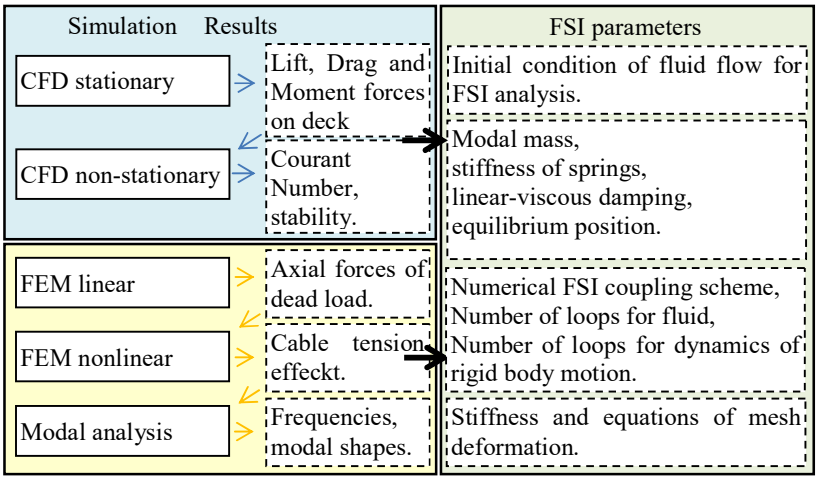

Figure 6: Scenario of FSI formulation ofaeroelastic phenomena

Simulation is made at$L/2$ ofthe main span of the bridge. Model is simplified for coordinate system of rigid body movement. Centre of mass and shear centre are in origin of the shear centre. Origin of inertia forces, spring forces, damping and aerodynamic forces are calculated on origin of coordinate system in shear centre.System of two degrees of freedom is simulated with rigid body formulation inAnsys*CEL language*; modal mass, viscos-elastic damper, and

linear spring are defined inFigure 8.Results in Figure 8are updated in each time, when the fluid flow is calculated, rigid body deformation is calculatedin next loop.

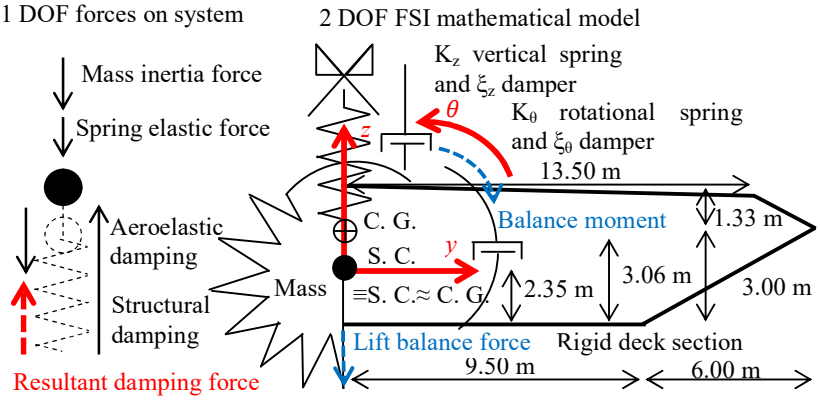

Figure 7: Mathematical model programmed in Ansys CEL language.

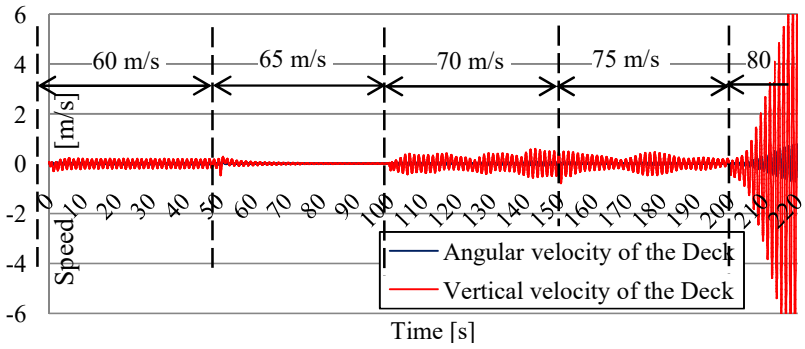

Figure 8: Aeroelastic response of the deck at the midpoint of the bridge.

Large oscillations occur when wind speed is around 80 m/s. Large rotational and vertical movement occur until mathematical model becomes unstable. Instability occurs when one of the control cells has negative volume and a simulation is stopped.

3.2.1 Finite element model

FEM was made in software SAP2000. Cables, pylons and deck were modelled as line elements. Cable deformation for dead load was calculated with SAP cable wizard program. Second order analysis was used for proper catching of tension stiffening effect of main cables. Because stiffness was calculated on deformed FEM model it is not correct. To match correct stiffness pre-tensioning of main cables on original position is done, so that dead load displacement is zero.

Dynamical properties are considered in Figure 9 for investigation of first symmetric vertical mode $\omega_z = 0.602 rad/s$and first symmetrical torsionalmode is$\omega_\theta = 1.836 rad/s$. At the centre of the bridge first symmetrical vertical and first symmetrical torsional mode were investigated at 1 m weight deck section.

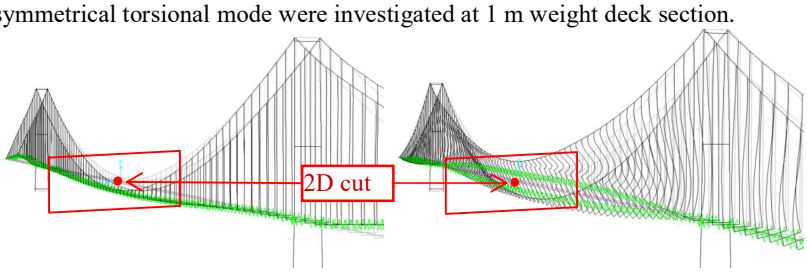

Figure 9:First symmetrical vertical mode 2and symmetrical torsional mode 39

Masses and springs for Fluid structure interaction are calculated from FEM model. Modal mass is calculated in for the unit length of FSI analysis$L_{FSI} = 1m$. FEA model has span between two nodes $L_{FEM} = 25.38\, m$. Spectral displacement normalized on mass matrixfrom eigenvectors gives activated mass in *i*-degree of freedom:

$$\mathrm{m}_i^{FSI} = \frac{L_{FSI}(\phi_i)^{-2}}{L_{FEM}} \tag{13}$$

4 Results and conclusion

In this paper all steps of evaluating flutter speed were presented. The main question was the critical wind speed for this system. Our main goal was to apply advanced numerical programs for fluid structure interaction to asses flutter speed. An example of Great Belt East Bridge was investigated to compeer results of two different methods. The critical wind speed was calculated in three different ways. Result of flutter derivatives from experimental data was compered to FSI calculated flutter derivatives and final result of flutter speed. The third way was the FSI analysis with the ANSYS software. The wind speed was increased step-by-step until the critical wind speed was found. Alternatively, considering the complexity of the problem, an approximation of 2D mesh and section in the middle of the bridge as rigid-body formulation was investigated. First the aerodynamic derivatives were extracted from a 2D CFD simulation and the critical wind speed was evaluated using an updated method afterwards. The critical wind speeds obtained with three different methods are in good agreement. The results of FSI simulation show slightly lower value of wind speed which seems to be good coincidence in this complex simulation. Naturally the inflow velocity steps should be more accurate in order to capture the flutter speed more precisely. In addition to that the 2D mesh should be extended into

3D mesh. Also multimodal response should be captured for correct estimation of flutter speed. Furthermore the method has potential for evaluating of flutter speed in phase of construction where no experimental data are available.

Extraction of flutter derivatives is in good agreement with experimental data. Critical wind speed from flutter derivatives from wind tunnel testing gives flutter speed 91m/s and flutter derivatives from FSI extraction gives final wind speed 97 m/s. Flutter speed from direct FSI analysis is around 80 m/s.

5 ACKNOWLEDGEMENTS

I am deeply grateful to Professors S. Hernandez, J. Á.Jurado and their colleges from Universityof La Coruña in Spain for their help. I owe my most sincere gratitude to my mentors J. K.Stajnko and A. Štrukelj for all their support.

References

[1]Matsumoto, M., Shirato, H., Yagi, T., Shijo, R.,Eguchi, A., Tamaki, H., Effects of aerodynamic interface between heaving and torsional vibration of the bridge decks: the case of Tacoma Narrows Bridge, *Journal of Wind Engineering and Industrial Aerodynamics*, 1547-1557,2003

[2]Scanlan, R.H., Airfoil and bridge deck flutter derivatives. Journal of Engineering Mechanics Division, ASCE. 97, 6, 1990

[3]Jurado J. A.,Hernández, S.,Theories of Aerodynamic Forces on Decks of Long Span Bridges. J. of Bridge Eng. 5, n1 8-13, 2000

[4]Le, T.H., Nguyen, D.A., Bridge aeroelasticy in frequency domain. Airfoil and bridge deck flutter derivatives, 1992
http://uet.vnu.edu.vn/~thle/Bridge%20aeroelastic%20analysis_notsubmit.pdf

[5]Starossek,U.,Brueckendynamik, Vieweg, Braunschweig/Germany.

[6]Starossek, U.,Prediction of bridge flutter through use of finite elements. *Structural Engineering Review*, Vol. 5, No. 4, pp. 301-307,1993

[7]Kenneth, S., Robert, S. Investigation on Long-span suspension bridges during erection, The Great Belt East Bridge, pp. 34.

[8]Kenneth, S., Robert, S. Investigation on Long-span suspension bridges during erection, The Great Belt East Bridge, pp. 32.

[9] Tanaka H., *Aeroelastic stability of suspension bridges during erection*. Structural Engineering International. Journal of the International Association for Bridge and Structural Engineering (IABSE). Vol. 8, No. 2, pp. 118–123,1998

[10]Ansys help tutorial for CFX 14, Ansys software for multiphasic computational dynamics, 2012